Laser Glazing of Plasma-Sprayed Zirconia Coatings

H.L. Tsai and P.C. Tsai

(Submitted 3 January 1995; in revised form 25 November 1997)

A CO_2 laser with cylindrical focal lens has been used to glaze the surface layer of plasma-sprayed ZrO_2 –20wt% Y_2O_3/MCrAlY coatings. Both a continuous-wave laser and a pulsed laser were used in this study. Different parameter settings for power, travel speed, and pulse frequency were used, and their effects on the melting width, melting depth, coupling efficiency, microstructure, surface roughness, and process defects have been evaluated. Results show that the melting width of the glazed track was slightly smaller than the diameter of the raw beam. The melting depth increased with increasing energy density for both a continuous-wave laser and a pulsed laser. The coupling efficiency as about 40 to 65% for a continuous-wave laser, which increased with increasing laser travel speed, but decreased with an increase in energy density. The power density has no significant effect on coupling efficiency. Defects, such as bubbles or depressions, occur easily with a continuous wave laser. A high-quality glazed layer is successfully produced using a pulsed laser. The surface roughness of the plasma-sprayed ceramic coatings was significantly improved by laser glazing. Surface roughness decreased slightly as the pulse frequency increased for the glazed surface. Based on this study, proper processing parameters have been suggested.

Keywords Co_2 laser glazing, plasma spray, process defects, processing parameter, pulsed laser, zirconia

1. Introduction

Previous research (Ref 1-4) showed that oxidation of the bond coat as well as thermal stresses were the main factors affecting the degradation of thermal barrier coatings (TBCs). Erosion (Ref 5, 6) and corrosion (Ref 7-9) are other factors contributing to TBC degradation. Presently, laser glazing is recognized as a promising process to solve these problems (Ref 10-15). This concept and the desired state of TBCs are described in Ref 16.

Several studies (Ref 10-21) have been conducted on the laser glazing of TBCs. Defects, including depressions, bubbles, and pinholes occurring in the glazed layer are the major problems found in these studies. These defects decrease the erosion resistance of TBCs. Also, a high-temperature corrosion test by Jasim et al. (Ref 20) showed that the depressions served as pockets for species concentration, thus leading to some preferential corrosion. Consequently, production of a defect-free glazed layer is desired. In an earlier study (Ref 22), the authors reported the effects of processing variables in laser glazing plasma-sprayed TBCs using a spherical focal lens. A region of appropriate processing parameters had been suggested. Results arising from earlier research on the laser glazing of plasma-sprayed TBCs using a cylindrical focal lens are presented.

2. Experimental Procedure

The substrates, 420 stainless steel coupons in the form of $100 \times 25 \times 2$ mm, were grit blasted with alumina powder to increase the adherence between the bond coat and the substrate. The specimens were first sprayed with Ni-22Cr-10Al-1Y bond coating and then with a ZrO_2-20wt%Y_2O_3 top coating in an air-plasma spray system. The spraying parameters are the same as those used in a previous study (Ref 16).

A CO_2 laser (10.6 μm wavelength) was used in this investigation. The raw beam was 16 mm in diameter. The fundamental transverse electromagnetic mode (TEM) of the laser was TEM_{00+01*}. The configuration of the laser system was the same as that used in a previous study (Ref 22), but with a minor modification—a cylindrical focal lens was used instead of a spherical one. The focal length of the focal lens was 127 mm. A line beam was obtained through this focal lens. The focus was set on the sample surface. Both a continuous-wave laser and a pulsed laser were used in this study. The pulsed model used a gated pulse. During laser glazing, an argon gas jet (at the flow rate of 10 L/min) was introduced to protect the lens and the melting surface. The travel direction was perpendicular to the line beam.

The width of the line beam, or spot size (abbreviated as $2W_f$), was calculated according to the previous study (Ref 23, 24). The incident power density (I_0) was calculated by Eq 1:

$$I_0 = \frac{P}{D \times 2W_f} \quad \text{(Eq 1)}$$

where P is the laser power, D is the diameter of the raw beam, and $2W_f$ is the spot size.

The interaction time (t_h) was calculated by the following equation:

$$t_h = \frac{2W_f}{F} \quad \text{(Eq 2)}$$

where F is the travel speed.

The energy density (E_{input}) was calculated by the following equation:

$$E_{\text{input}} = d\,\frac{P}{FW} \quad \text{(Eq 3)}$$

H.L. Tsai and **P.C. Tsai,** Department of Mechanical Engineering and Technology, National Taiwan Institute of Technology, Taipei, Taiwan, 10772, ROC.

where P is the laser power, d is the duty of the pulse, F is the travel speed, and W is the melting width. The coupling efficiency was calculated with a value of q_0/I_0 taken from Greenwald et al. (Ref 25).

After laser glazing, the width of the glazed region was measured with a micrometer. An optical microscope was used to examine the transverse sections of the microstructure. A scanning electron microscope (SEM) was used to study the effects of laser parameters on the melting depth, transverse sectional microstructure, and surface appearance. X-ray diffractometry (XRD) was used to characterize the crystal structure of the glazed layer. Roughness measurements on the surface were made parallel to the melted track.

3. Results and Discussion

3.1 Continuous Wave Laser

Melting Width. When a line beam is created using a laser with a cylindrical focal lens, glazing occurred perpendicular to the line beam. Theoretically, the melting width should be equal to the diameter of the raw beam (that is, 16 mm). The melting width of the glazed track was slightly smaller than the diameter of the raw beam (Ref 11). The slight discrepancy, attributable to differing energy density, is negligible and does not warrant further elaboration.

Melting Depth and Coupling Efficiency. An acrylic resin specimen was laser irradiated using varying laser powers. When the power exceeded 1000 W, it created a noticeably uneven burn pattern. Thus, in this section, discussion will center on evaluating the melting depth and coupling efficiency obtained with a maximum laser power of 1000 W.

As shown in Fig. 1, the melting depth increased with increasing energy density. As the energy density reached 7.5 J/mm^2, the melting depth reached approximately 170 μm. Figure 1 also shows the relationship between coupling efficiency and energy density. The coupling efficiency is approximately 30 to 65% and decreases as energy density increases.

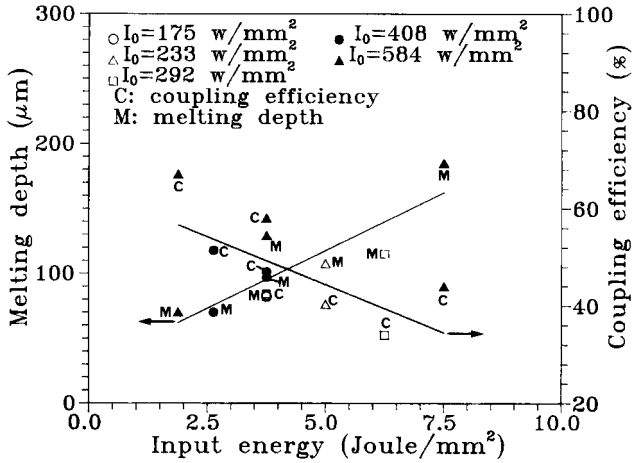

Fig. 1 Melting depth and coupling efficiency as a function of energy density, continuous-wave laser

Figure 2 shows the relationship between coupling efficiency and travel speed, with the former increasing as the latter increases. The results of this study demonstrate that the use of a cylindrical focal lens produced a higher coupling efficiency than the use of a spherical focal lens (Ref 22). This is due to the fact that the former was glazed on its focal place and thus its power density was higher and the line beam was narrow, whereas the latter was farther from its focal plane and thus the diameter of the laser beam was larger. Even with a slower travel speed, the interaction time would be considerably less for the former, which would result in a decrease of plasma plumes as well as increased coupling efficiency. The formation and effects of plasma plumes will be discussed in detail in Section 3.2.

Process Defects. The effect of the varying parameters used in this study are shown in Fig. 3. When a comparatively low power is used (as indicated by the area below the dotted line in

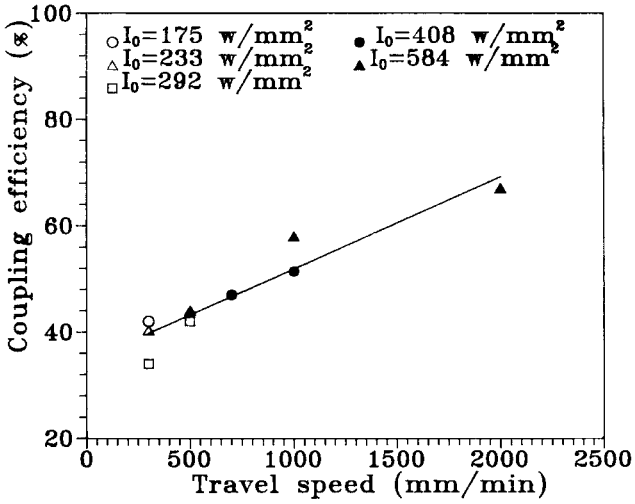

Fig. 2 Relationship between coupling efficiency and travel speed, continuous-wave laser

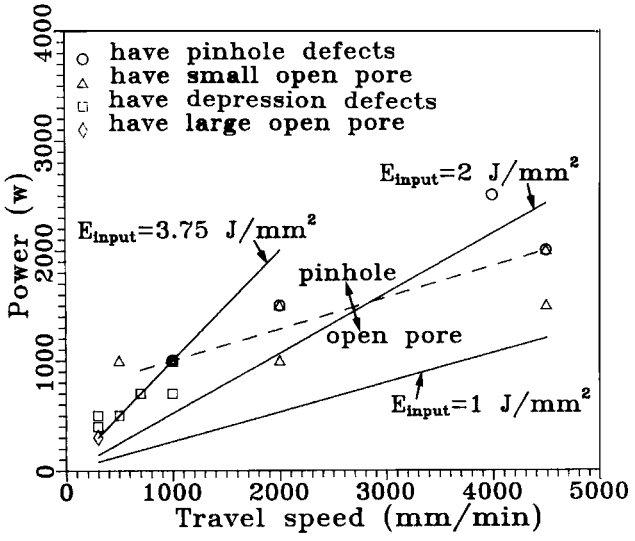

Fig. 3 Operational parameters for continuous-wave laser glazing obtained by a combination of laser power and travel speed

Fig. 3), the glazed surface developed open pores, which proliferate at a slow travel speed and low power level.

Figure 4(a) shows the numerous open pores spread over the glazed surface, which was glazed using a laser power of 300 W at speeds of 300 mm/min. Figure 4(b), in addition to illustrating the prevalence of open pores, also reveals partially closed pores (arrow) with diameters of approximately 100 μm. These pores appeared on the glazed surface as it solidified, occurring primarily because as the glazed surface melted, porosities became trapped and were unable to rise due to the lower temperature of the melting layer, which had a higher viscosity.

The open pores described above can be markedly repressed if the laser power is increased or if the travel speed of the test

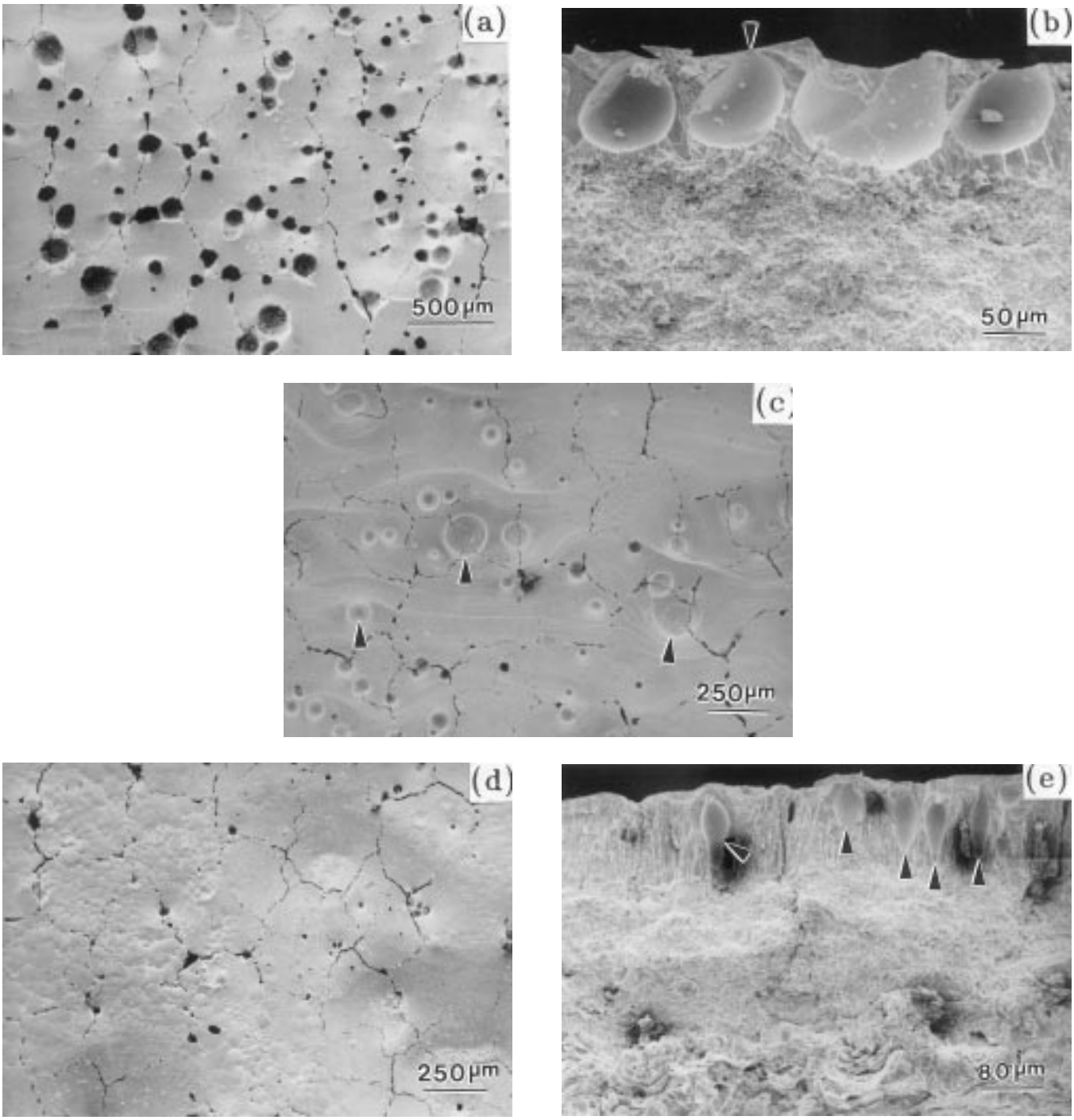

Fig. 4 Scanning electron micrographs showing the process defects, continuous-wave laser. (a) and (b) Open pore and closed pore defects obtained with 300 W and 300 mm/min. (a) Top view. (b) Cross-sectional view. (c) Depression defects obtained at 1000 W and 2000 mm/min, top view. (d) and (e) Surface nucleation and pinhole defects obtained at 2000 W and 4500 mm/min. (d) Top view and (e) cross-sectional view

specimen is simultaneously increased. Shallow depressions occur on a surface glazed in such a manner, as illustrated by the typical SEM microstructures shown in Fig. 4(c). These shallow depressions are far fewer in number than the open pores.

If a laser with an even higher power density is used (as indicated by the area above the dotted line in Fig. 3), the laser-glazed surface is marked by small open pores. The microstructures for this phenomenon are illustrated in Fig. 4(d), and the pinhole defects are clearly visible in the cross-sectional view of Fig. 4(e). The formation of pinhole defects was the result of surface nucleation. It is thus clear that the use of power (i.e., power density) set at excessive levels in the glazing process also yields unsatisfactory results.

From the above discussion, it can be seen that by using a cylindrical focal lens with a continuous-wave laser, it is almost impossible to achieve a glazed surface free from defects. To eradicate these pores, a double-pass glazing process was used in this study, whereby a lower energy density was applied along the same track of a freshly glazed specimen by lowering the laser power density or increasing the travel speed. Although these methods can achieve a surface that is free of open pores of pinholes, the glazed surface experienced delamination. Figure 5(a) illustrates the delamination (arrow), and Fig. 5(b) shows delamination occurring on the glazed layer/HAZ interface. It is thus obvious that the use of the double-pass method also produces unacceptable results.

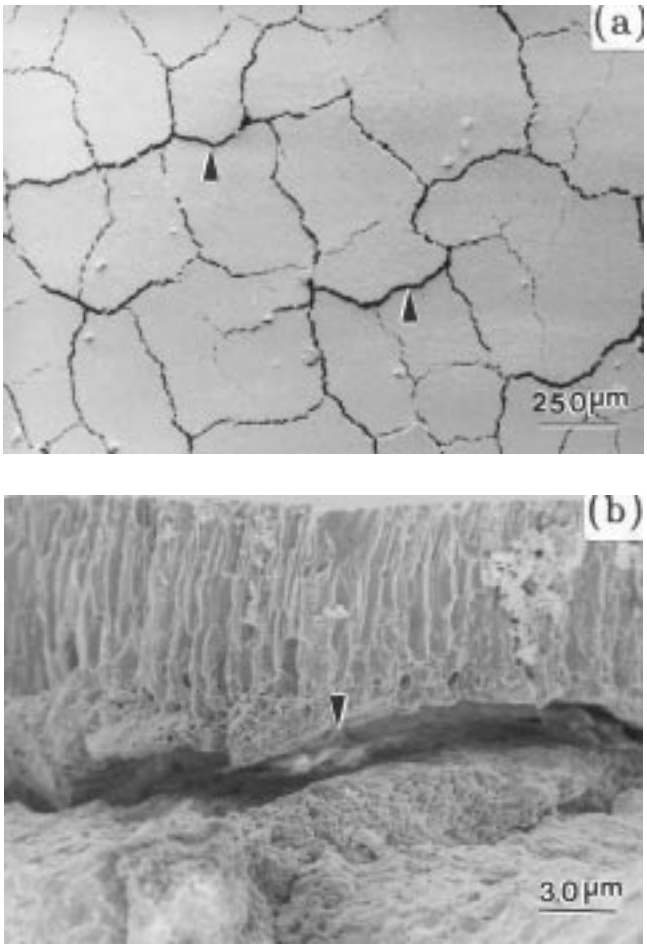

Fig. 5 Superimposed laser glazing showing delamination of glazed layer, continuous-wave laser. (First pass: 700 W and 1000 mm/min; second pass: 500 W and 1000 mm/min). (a) Top view. (b) Cross-sectional view

3.2 Pulsed Laser

Melting Depth and Coupling Efficiency. Figure 6 shows that the melting depth increases in proportion to the energy density. When the energy density increased to 1.5 J/mm^2, the melting depth reached 110 μm. Comparing these results to those in Fig. 1, it can be seen that a melting depth of approximately 100 μm does not occur until an energy density of 3.75 J/mm^2 from a continuous laser beam is used. This implies that the coupling efficiency of a pulsed laser is higher than that for

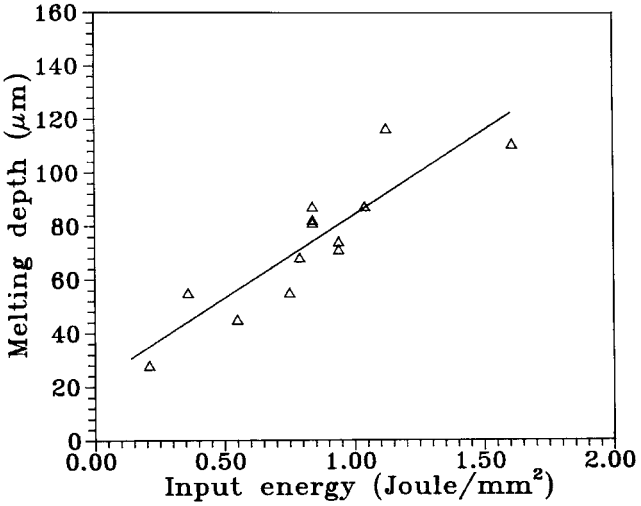

Fig. 6 Relationship between melting depth and energy density, pulsed laser

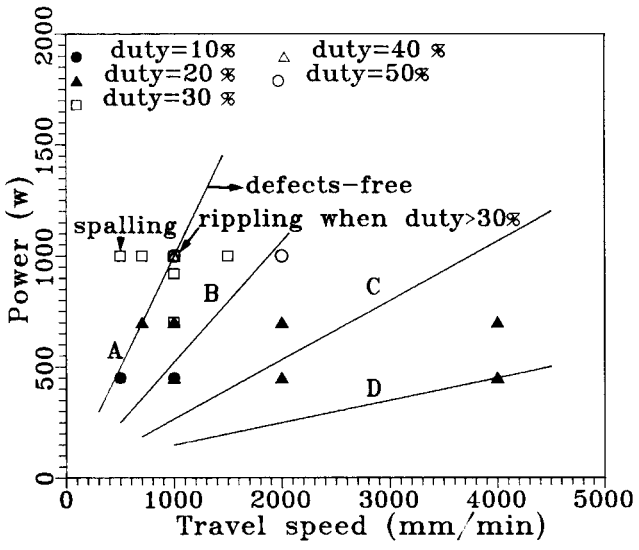

Fig. 7 Defect-free glazing conditions obtained by a combination of laser power and travel speed, pulsed laser. A: E_{input}/duty = 3.75 J/mm^2. B: E_{input}/duty = 2 J/mm^2. C: E_{input}/duty = 1 J/mm^2. D: E_{input}/duty = 0.675 J/mm^2

a continuous beam laser. Due to the nature of a pulsed laser, the areas melted by one pulse overlap those of subsequent pulses, a situation that results in preheating. Therefore, use of a q_0/I_0 model to estimate coupling efficiency is not feasible.

Defect-Free Glazing Parameters. Figure 7 shows the defect-free glazing region based on parameters of laser power and the specimen travel speed. Spalling occurred only when the value of E_{input}/duty was larger than 3.75 J/mm^2. A defect-free glazed layer was obtained when the value of E_{input}/duty did not exceed 3.75 J/mm^2. As shown in Fig. 7, the appropriate processing parameters of 450 to 1000 W laser power and 500 to 4000 mm/min travel speed are suggested. As indicated in Fig. 3, it is difficult to obtain a good glazed layer using such parameters for a continuous-wave laser.

The appropriate glazing parameters for the pulse duty and energy density show that the most suitable pulse duty is 10 to 30%, with an energy density of 0.15 to 1.6 J/mm^2; delamination of the glazed layer occurs in the HAZ if energy density is too great; rippling also occurs on the glazed surface if the pulse duty is too high. Anthony et al. (Ref 26) noted that rippling is often caused by surface-tension gradients resulting from temperature gradients.

Figure 8 shows the scanning electron microstructures of glazed coatings obtained with different frequencies. The size of the segmented blocks do not undergo significant change, even when the pulse rate is changed. The effects of such laser glazing are shown in Fig. 8. Depressions found in Fig. 8(a) have all disappeared, as shown in Fig 8(b) and (c). Disappearance of the defects is mainly attributed to the use of the pulsed laser and through ready occurrence of plasma plumes.

For example, the interaction time of a continuous-wave laser with a power rate of 700 W and a travel speed of 1000 mm/min is calculated to be 6.4 ms. On the other hand, the pulsing time for each pulse is calculated as 0.75 ms if a pulsed laser with parameters of 400 Hz and 30% duty is used. Obviously, it is difficult to induce the occurrence of plasma plumes using pulsed laser. Ready (Ref 27) found that when a MgO material was irradiated by a laser beam, which induced approximately four cycles of plume generation, decoupling, plume dissipation, and recoupling occurred during the 5-ms pulse. Although plasma plumes that occurred in ZrO_2 were different from those in MgO, at 0.75-ms pulses, plasma plumes rarely occurred. Previous study (Ref 28-30) showed that the existence of plasma plumes created an impinging force that made it difficult for bubbles to escape. The plumes also made it impossible for the laser to penetrate and caused coupling efficiency to decrease, thereby making it impossible for a glazed surface to reach higher temperatures. The temperature of the melt was

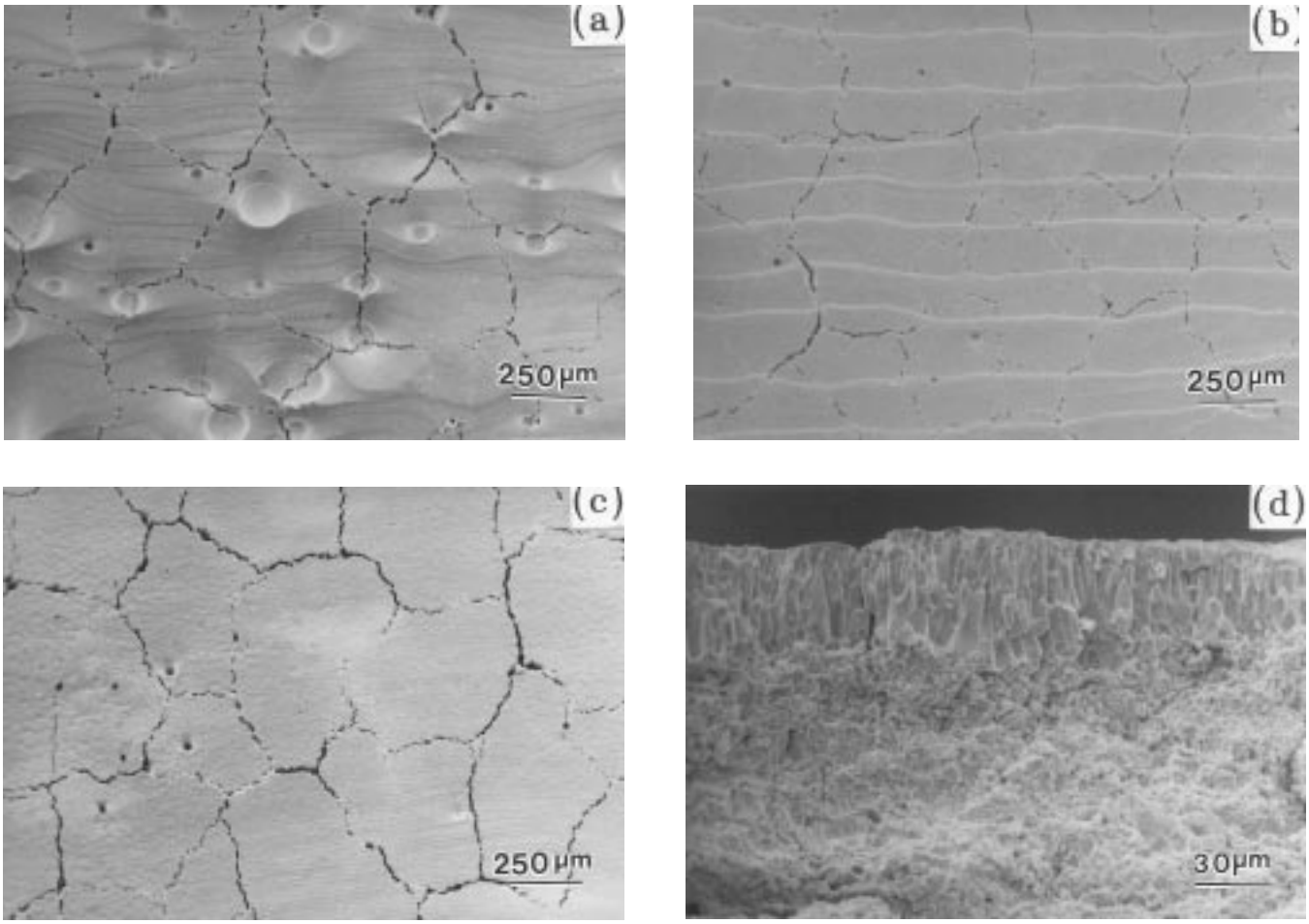

Fig. 8 Scanning electron micrographs of as-glazed top coat showing the effect of pulsed laser, 700 W and 1000 mm/min. (a) Continuous-wave laser. (b) 20% duty, 100 Hz. (c) 30%duty, 800 Hz. (d) Cross-sectional view of (b)

low and the viscosity was even higher. Both of these mechanisms made it difficult for bubbles to escape, instead remaining on the glazed layer. Use of a pulsed laser improved this condition and made it difficult for either bubbles or depressions to occur.

Figure 8(b) and (c) also illustrate the ripples created by each pulse of the laser, which may have been caused by surface-tension gradients. The roughness value (Ra) for the surface of the as-sprayed coating was 8.7 μm. The value for the surfaces in Fig. 8(a), (b), and (c) were 5.1, 5.2, and 3.5 μm, respectively. When the pulse frequency was 100 to 800 Hz, surface roughness decreased slightly as the pulse frequency increased. Obviously, after being laser glazed, there was a significant improvement in roughness on the glazed surface.

Figure 8(d) shows a cross-sectional scanning electron micrograph of Fig. 8(b). The microstructures of all samples glazed using defect-free parameters are similar. Depressions and defects are not found in the glazed layer. The findings in this article have shown that pulse frequencies between 100 to 800 Hz can achieve a quality glazed surface.

4. Conclusions

Plasma-sprayed ZrO_2–20 wt% Y_2O_3/MCrAlY coatings have been glazed by the use of a CO_2 laser with a cylindrical focal lens. Both continuous-wave and pulsed lasers were used in this study. The effects of laser parameters on the melting width, melting depth, coupling efficiency, microstructure, and process defects were evaluated. The conclusions of this study can be summarized as follows.

The melting width of the glazed track was slightly smaller than the diameter of the raw beam (that is, 16 mm). The melting depth increases with increasing energy density for both a continuous-wave laser and a pulsed laser. The coupling efficiency is about 40 to 70% for the continuous-wave laser, which increased with increasing laser travel speed, but decreased with an increase in energy density. The power density had no significant effect on coupling efficiency. The surface roughness of the plasma-sprayed ceramic coating improved significantly with laser glazing. The roughness value decreased slightly with increasing pulse frequency. Use of a pulsed laser prevented defect formation, which occurred easily with a continuous-wave laser. The appropriate processing parameters are suggested.

Acknowledgments

Financial support from the National Science Council (No. NSC 81-0405-E-011-06) of the Republic of China (Taiwan) is acknowledged. The authors would also like to express their appreciation to Dr. David C. Tu, Vice President of Mooney Co. Ltd., Taipei, for his kind assistance.

References

1. R.A. Miller and C.E. Lowell, Failure Mechanisms of Thermal Barrier Coatings Exposed to Elevated Temperatures, *Thin Solid Films*, Vol 95, 1982, p 265-273
2. C.C. Berndt and H. Herman, Failure During Thermal Cycling of Plasma-Sprayed Thermal Barrier Coatings, *Thin Solid Films*, Vol 108, 1983, p 427-437
3. A. Bennett, Properties of Thermal Barrier Coatings, *Mater. Sci. Technol.*, Vol 2 (No. 5), 1986, 257-261
4. B.C. Wu, E. Chang, S.F. Chang, and D. Tu, Degradation Mechanisms of ZrO_2–8wt%Y_2O_3/Ni-22Cr-10Al-1Y Thermal Barrier Coatings, *J. Am. Ceram. Soc.*, Vol 72 (No. 2), 1989, p 212-218
5. J.W. Wogan, L. Hsu, and A.R. Stetson, Thermal Barrier Coatings for Thermal Insulation and Corrosion Resistance in Industrial Gas Turbine, *Thin Solid Films*, Vol 84, 1981, p 75-87
6. A.G. Davis, D.H. Boone, and A.V. Levey, Erosion of Ceramic Thermal Barrier Coatings, *Wear*, Vol 110, 1986, p 101-116
7. R.J. Bratton and S.K. Lau, Zirconia Thermal Barrier Coatings, in *Advances in Ceramics*, Vol 3, A.H. Heuer and L.W. Hobbs, Ed., The American Ceramic Society, Columbus, OH, 1981, p 226-240
8. R.L. Jones and C.E. Williams, Hot Corrosion Studies of Zirconia Ceramics, *Surf. Coat. Technol.*, Vol 32, 1987, p 349-358
9. J.T. Prater and E.L. Courtright, Ceramic Thermal Barrier Coatings with Improved Corrosion Resistance, *Surf. Coat. Technol.*, Vol 32, 1987, p 389-397
10. R.A. Miller and C.C. Berndt, Performance of Thermal Barrier Coatings in High Heat Flux Environments, *Thin Solid Films*, Vol 119, 1984, p 195-202
11. H.L. Tsai and P.C. Tsai, Thermal Cyclic Response of Laser Glazed Plasma Sprayed (ZrO_2-19.5 wt% Y_2O_3)/(Ni-22Cr-10Al-1Y) Thermal Barrier Coatings., *Mater. Sci. Eng.*, Vol A177, 1994, p 227-232
12. P.C. Tsai, H.L. Tsai, and D.C. Tu, Laser Glazing of Plasma Sprayed Thermal Barrier Coatings and Its Effect on High Temperature Cyclic Oxidation Behaviour, *Proc. 1992 Ann. Conf. Chinese Mater. Sci.*, Chinese Society for Materials Science, Taipei, Taiwan, R.O.C., 1992, p 576-577
13. A. Adamski and R. McPherson, Laser Processing of Thermally Sprayed Coatings, in *Advances in Thermal Spraying, Proc. Int. Thermal Spraying Conf.*, Welding Institute of Canada, Pergamon Press, New York, 1986, p 555-562
14. I. Zaplatynsky, Performance of Laser-Glazed Zirconia Thermal Barrier Coatings in Cyclic Oxidation and Corrosion Burner Rig Tests, *Thin Solid Films*, Vol 95, 1982, p 275-284
15. R. Sivakumar and B.L. Mordike, Laser Melting of Plasma Sprayed Ceramic Coatings, *Surf. Eng.*, Vol 4 (No. 2), 1988, p 127-140
16. H.L. Tsai, P.C. Tsai, and D.C. Tu, Characterization of Laser Glazed Plasma Sprayed Yttria Stabilized Zirconia Coatings, *Mater. Sci. Eng.*, Vol A161, 1993, p 145-155
17. N. Iwamoto, N. Vmesaki, Y. Katayama, and H. Kuroki, Surface Treatment of Plasma-Sprayed Ceramic Coatings by a Laser Beam, *Surf. Coat. Technol.*, Vol 34, 1988, p 59-67
18. G.S. Fischman, C.H. Chen, J.M. Rigsbee, and S.D. Brown, Character of Laser-Glazed, Plasma-Sprayed Zirconia Coatings on Stainless Steel Substrate, *Ceram. Eng. Sci. Pro.*, Vol 9, 1985, p 908-918
19. K.M. Jasim, D.R.F. West, W.M. Steen, and R.D. Rawlings, Laser Surface Sealing of Plasma Sprayed Yttria Stabilized Zirconia Ceramics, in *Laser Materials Processing, Proc. Int. Conf. On ALEO, 1988*, G. Brock, Ed., Laser Institute of America, Toledo, OH, 1989, p 17-31
20. K.M. Jasim, R.D. Rawlings, and D.R.F. West, Pulsed Laser Processing of Thermal Barrier Coatings, *J. Mater. Sci.*, Vol 26, 1991, p 909-916
21. K.M. Jasim, R.D. Rawlings, and D.R.F. West, Characterization of Plasma-Sprayed Layers of Fully Yttria-Stabilized Zirconia Modified by Laser Sealing, *Surf. Coat. Technol.*, Vol 53, 1992, p 75-86
22. P.C. Tsai, H.L. Tsai, and D.C. Tu, Study of Processing Variables in Laser Glazing Plasma-Sprayed Thermal Barrier Coatings, *Mater. Sci. Eng.*, Vol A165, 1993, p 167-173

23. J.T. Luxon, Optics for Materials Processing, in *Industrial Laser Materials Processing 1986/1987*, D. Belforte and M. Levitt, Ed., Pen Well, Tulsa, OK, 1988, p 16-26

24. J. Meijer, M. Seegers, P.H. Vroegop, and J.W. Wes, Line Hardening by Low-Power CO_2 Lasers, in *Laser Welding, Machining and Materials Processing, Proc. Int. Conf. Appl. Lasers and Electro-Optics, 1985*, C. Albright, Ed., IFS Ltd., Bedford, UK, 1986, p 229-238

25. L.E. Greenwald, E.M. Breinan, and B.H. Kear, Heat Transfer Properties and Microstructures of Laser Surface Melted Alloys, in *Laser-Solid Interactions and Laser Processing 1978*, S.P. Ferris, H.J. Leamy, and J.M. Poate, Ed., American Institute of Physics, New York, 1979, p 189-204

26. T.R. Anthony and H.E. Cline, Surface Rippling Induced by Surface-Tension Gradients During Laser Surface Melting and Alloying, *J. Appl. Phys.*, Vol 48 (No. 9), 1977, p 3888-3894

27. J. Ready, Interaction of High-Power Laser Radiation with Materials, *Industrial Application Lasers*, J. Ready Ed., Academic Press, New York, 1978, p 336-357

28. G.K. Lewis and R.D. Dixon, Plasma Monitoring of Laser Beam Welds, *Weld. J.*, Vol 64 (No. 2), 1985, p 49s-54s

29. A.N. Pirri, R.G. Root, and K.S. Wu, Plasma Energy Transfer to Metal Surfaces Irradiated by Pulsed Lasers *AIAA J.*, Vol 16 (No. 12), 1978, p 1296-1304

30. T.H. Kim, Porosity Formation in Laser-Beam Materials Processing, *J. Mater. Sci. Lett.*, Vol 10, 1991, p 400-402